



Delft University of Technology

The relationship between inundation duration and *Spartina alterniflora* growth along the Jiangsu coast, China

Li, Runxiang; Yu, Qian; Wang, Yunwei; Wang, Zhengbing ; Gao, Shu; Flemming, Burg

DOI

[10.1016/j.ecss.2018.08.027](https://doi.org/10.1016/j.ecss.2018.08.027)

Publication date

2018

Document Version

Final published version

Published in

Estuarine, Coastal and Shelf Science

Citation (APA)

Li, R., Yu, Q., Wang, Y., Wang, Z., Gao, S., & Flemming, B. (2018). The relationship between inundation duration and *Spartina alterniflora* growth along the Jiangsu coast, China. *Estuarine, Coastal and Shelf Science*, 213, 305-313. <https://doi.org/10.1016/j.ecss.2018.08.027>

Important note

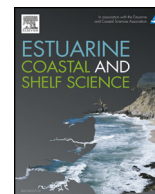
To cite this publication, please use the final published version (if applicable). Please check the document version above.

Copyright

Other than for strictly personal use, it is not permitted to download, forward or distribute the text or part of it, without the consent of the author(s) and/or copyright holder(s), unless the work is under an open content license such as Creative Commons.

Takedown policy

Please contact us and provide details if you believe this document breaches copyrights. We will remove access to the work immediately and investigate your claim.



The relationship between inundation duration and *Spartina alterniflora* growth along the Jiangsu coast, China



Runxiang Li^a, Qian Yu^{b,*}, Yunwei Wang^{c,**}, Zheng Bing Wang^{a,d}, Shu Gao^e, Burg Flemming^f

^a Faculty of Civil Engineering and Geosciences, Delft University of Technology, Stevinweg 1, 2624 GA Delft, The Netherlands

^b MOE Laboratory for Coast and Island Development, Nanjing University, 210093 Nanjing, China

^c College of Harbor, Coastal and Offshore Engineering, Hohai University, Nanjing, China

^d Deltares, 2600 MH Delft, The Netherlands

^e State Key Laboratory of Estuarine and Coastal Research, East China Normal University, Shanghai 200062, China

^f Senckenberg Institute, Wilhelmshaven D-26382, Germany

ARTICLE INFO

Keywords:

Spartina alterniflora
Above-ground biomass
Inundation duration
Jiangsu coast
China

ABSTRACT

The above-ground biomass of *Spartina alterniflora* salt marsh meadows is influenced by numerous interacting factors, among them elevation, tidal range and inundation duration. Bio-geomorphological models make use of either linear or quadratic equations, but it is important to be aware that the variables are area specific and hence not generic. In order to explore the vegetation growth pattern and its influencing factors along the Jiangsu coast, China, field surveys were conducted in two typical *S. alterniflora* marshes along the coast of Dafeng and Rudong. To combine the influence of elevation and the effect of tidal range, the inundation ratio (*IR*) is introduced as a novel parameter, which is the ratio between inundation duration and the duration of the whole tidal period concerned. The relationship between above-ground biomass and *IR* can be expressed by a quadratic equation. The optimal inundation ratio for *S. alterniflora* along the Jiangsu coast ranges from 0.21 to 0.26, which is much lower than, for example, that for the marsh of North Inlet (0.35), South Carolina, and the Virginia Coast Reserve (0.41), USA. Tidal range plays a significant role in that a larger tidal range leads to a smaller optimal *IR*, and that the landward and seaward limits are displaced toward higher ground elevations. In macrotidal regions the submergence depth is larger, which results in enhanced submergence and salinity stress for the entire marsh, causing it to shift toward higher elevations. Tidal range is an important factor influencing the growth pattern of *S. alterniflora*, but geomorphological factors such as topographic profiles, and the presence of cliffs and tidal creeks must also be taken into account.

1. Introduction

Salt marshes are one of the most productive ecosystems in the world (Gallagher et al., 1980), providing numerous habitats to vertebrate and invertebrate faunas, and being an invaluable natural resource to coastal residents. Marsh vegetation protects the coast from storm surges by dissipating wave energy, reducing tidal currents, enhancing sediment retention and accelerating tidal flat expansion (Allen, 2000; Temmerman et al., 2013; Gao et al., 2014). Because of these ecosystem services, the response of coastal marshes to sea-level rise has become an important research topic. Sea-level rise leads to longer time periods over which suspended sediments can deposit (Friedrichs and Perry, 2001). At the same time, longer submergence increases soil anoxia, which may eventually exceed the tolerance of halophytes (Bertness and

Ellison, 1987; Morris et al., 2002; Voss et al., 2013) and the balance between rates of sea-level rise and accretion rates determines whether salt marshes can survive a rise in sea level (Morris et al., 2002; Mudd et al., 2010; Kirwan et al., 2016a,b).

Both organic and inorganic deposition contributes to salt marsh accretion. The amount of deposition is, amongst others, related to various properties of the vegetation, in particular biomass, stem density, stem diameter and leaf area. Organic deposition is directly related to the vegetation biomass. Inorganic deposition includes sediment trapping by vegetation and direct settling on the salt marsh surface. Sediment trapping by vegetation is determined by leaf area and the projected total area (Yang, 1998; Chen et al., 2018). Sediment settling can be enhanced by vegetation because it decreases flow velocity and turbulence (Shi et al., 1995; Bouma et al., 2007; Nepf, 2012; Chen et al.,

* Corresponding author.

** Corresponding author.

E-mail addresses: qianyu.nju@gmail.com (Q. Yu), ms.ywwang@gmail.com (Y. Wang).

2016), and also dampens wave action (Wang et al., 2009; Feagin et al., 2011; Yang et al., 2012). Projected stem area and stem diameter, which are the main parameters from which the damping effect of vegetation is calculated, are both related to biomass (Morris and Haskin, 1990), which is thus a good proxy from which to estimate the effect of vegetation on fluid and sediment. Biomass or vegetation density are therefore the most widely used parameters in bio-geomorphological modeling (Mudd et al., 2004; Morris, 2006; D'Alpaos et al., 2007; Kirwan and Murray, 2007; Mariotti and Fagherazzi, 2010; Mudd et al., 2010).

Vegetation growth is limited by the flooding frequency and duration due to raised soil salinity and anoxia (Phleger, 1971; Naidoo et al., 1992; Morris, 1995; Wijte and Gallagher, 2013), indicating that the elevation of a marsh determines the flooding condition of the vegetation. Morris et al. (2002) found that the above-ground biomass (B) of *Spartina alterniflora* (*S. alterniflora*) in North Inlet, South Carolina (USA), is related to the depth below mean high tide (D) by the following relationship:

$$B = aD^2 + bD + c \quad (1)$$

where a , b and c are numerical values relating to the form of the regression.

The above-ground biomass has a hump-shaped cross-shore pattern in that it increases with decreasing elevation, reaches a maximum at the optimal elevation, and then decreases as the elevation drops below the optimal level. There is commonly an upper and a lower elevation limit between which *S. alterniflora* can survive (e.g., Gray, 1992). The seaward limit is determined by soil anoxia due to excessive submergence (Naidoo et al., 1992; Wijte and Gallagher, 2013). Toward the landward end of the marsh, the decreasing submergence rate leads to high evapotranspiration and increased soil salinity, which is ultimately fatal to halophytes (Phleger, 1971; Morris, 2000). Although the data from North Inlet only covered the area above optimal elevation (Morris et al., 2002), eq. (1) also predicts the area below optimal elevation. This predictive potential was shown to be correct by other investigations (Kirwan et al., 2012). Nevertheless, in some cases, geomorphological models have also made use of parabolic equations (Morris, 2006; Kirwan and Murray, 2007; Mariotti and Fagherazzi, 2010; Hagen et al., 2013; Alizad et al., 2016; Rodriguez et al., 2017).

Because the data of Morris et al. (2002) only cover the rising part of the hump-shaped curve, a linear relationship is often used to describe the spatial pattern of the vegetation (Mudd et al., 2004, 2009, 2010; D'Alpaos et al., 2005, 2007):

$$B = \left(\frac{z_{\max} - z_b}{z_{\max} - z_{\min}} \right) B_{\max} \quad \text{for } z_{\min} \leq z_b \leq z_{\max} \quad (2)$$

where z_b is the local marsh elevation, B_{\max} the maximum biomass, z_{\max} and z_{\min} the growth limits of the marsh. This linear equation provides a simple and efficient prediction, and is therefore particularly useful for modeling purposes, especially if the marsh is located above the optimal elevation. As pointed out by Morris (2006), the choice of a biomass model and associated variables should always be based on the site-specific (regional) conditions.

In fact, elevation is not the only determining factor of marsh biomass distribution. Also landform, tidal range and latitude can influence the vegetation pattern (e.g., Gray, 1992). Due to the presence of tidal creeks, the flooding duration increases near the tidal creeks. Tidal range may also influence marsh distribution by altering the growth range of the vegetation. In fact, growth range was found to be proportional to tidal range (McKee and Patrick, 1988; Balke et al., 2016). Whereas the landward limit of a salt marsh is influenced by latitude and species competition, the seaward (i.e. lower) limit is determined by the tolerance to submergence, salinity and anoxia (McKee and Patrick, 1988). Because the tidal range differs at different geographic locations, a unifying proxy is needed to identify the effect of hydrodynamic condition and geomorphology on vegetation. The non-dimensional depth is calculated by the ratio of the difference between mean high water level

(MHW) and the bed elevation to the mean tidal range. It is a useful proxy of the submergence intensity and easy to calculate (Morris et al., 2013; Alizad et al., 2016). The rising or lowering rate of water level is not constant during the tidal cycle. The rate is maximum at the middle of flood and ebb, while the rate is minimum at high or low water. Therefore, the actual submergence duration is not linear to non-dimensional depth. The non-dimensional depth may generate deviations from the actual submergence duration.

The inundation ratio (IR) is based on the actual submergence duration and thus has the direct physical meaning. IR, which is the ratio between inundation duration and the whole time span of the associated tidal cycles, is here proposed for that purpose. In practice, and assuming the relevant time span covers n tidal cycles and is long enough to remove the spring-neap variation, IR can be defined as:

$$IR = \frac{\sum_{i=1}^n t_i}{T} \quad (3)$$

where t_i is the inundation duration in the i th tidal cycle and T is the duration of total n tidal cycles. By this definition, the effects of tidal range and bed elevation are merged into a single predictive parameter (cf. also Bockelmann et al., 2002; Mudd et al., 2004).

The variables need to be determined regionally by using the biomass model to predict the marsh pattern. Morris et al. (2002) obtained the variables by performing long-term monitoring of the salt marsh in the North Inlet estuary, South Carolina, USA. Interestingly, Kirwan et al. (2012) derived the same equation on the basis of different variables derived from observations in the Virginia Coast Reserve, USA. This suggests that, due to regional differences in environmental conditions, more *in situ* investigations are required in geographically different regions in order to explore the comparability of the interaction between vegetation and geomorphology on a global scale.

Although *S. alterniflora* is a native species to the east coast of America, it has been introduced to China in 1979. Since then it has spread widely, especially along the coast of Jiangsu Province. The reason for its introduction to the Jiangsu coast was for the purpose of coastal protection and the claim of new land (Chung and Zhuo, 1985; Chen et al., 2004, 2005; Zhang et al., 2004). The broad and flat expanses of the tidal flats along the Jiangsu coast provide excellent habitats for *S. alterniflora* and it is thus not surprising that research on the evolution of *S. alterniflora* salt marshes from originally bare tidal flats has a high priority in China (Zhang et al., 2004; Zuo et al., 2013; Gao et al., 2014). Within this context, our research has the following three purposes: (a) to generate the local salt marsh variables for geomorphological modeling in order to assess the effects of future sea-level rise and land claims; (b) to explore the effects of geomorphology and tidal range on salt marsh vegetation growth; and (c) to contribute to the worldwide *S. alterniflora* salt marsh data base with the aim of establishing a universal salt marsh model.

2. Methods

2.1. Study area

As study two *S. alterniflora* marshes were chosen, one located in Dafeng, the other in Rudong, both located in the middle sector of the Jiangsu coast, China (Fig. 1). Due to the sediment supply of the Subei Coastal Current and nearshore residual currents influenced by the abandoned Yellow River Delta, the coast-normal profile is characterized by a wide and gentle slope, the tidal flat being composed of fine-grained sediment. The tidal regimes in Dafeng and Rudong are irregular semi-diurnal with average tidal ranges of 3 m and 4.5 m respectively (Ren, 1986; Wang et al., 2012). The Dafeng coast is relatively more exposed compared to Rudong, the longer fetch and more open environment leading to stronger wind-wave influence in the former case, where the annual mean significant wave height is 0.48 m (measured at the B1

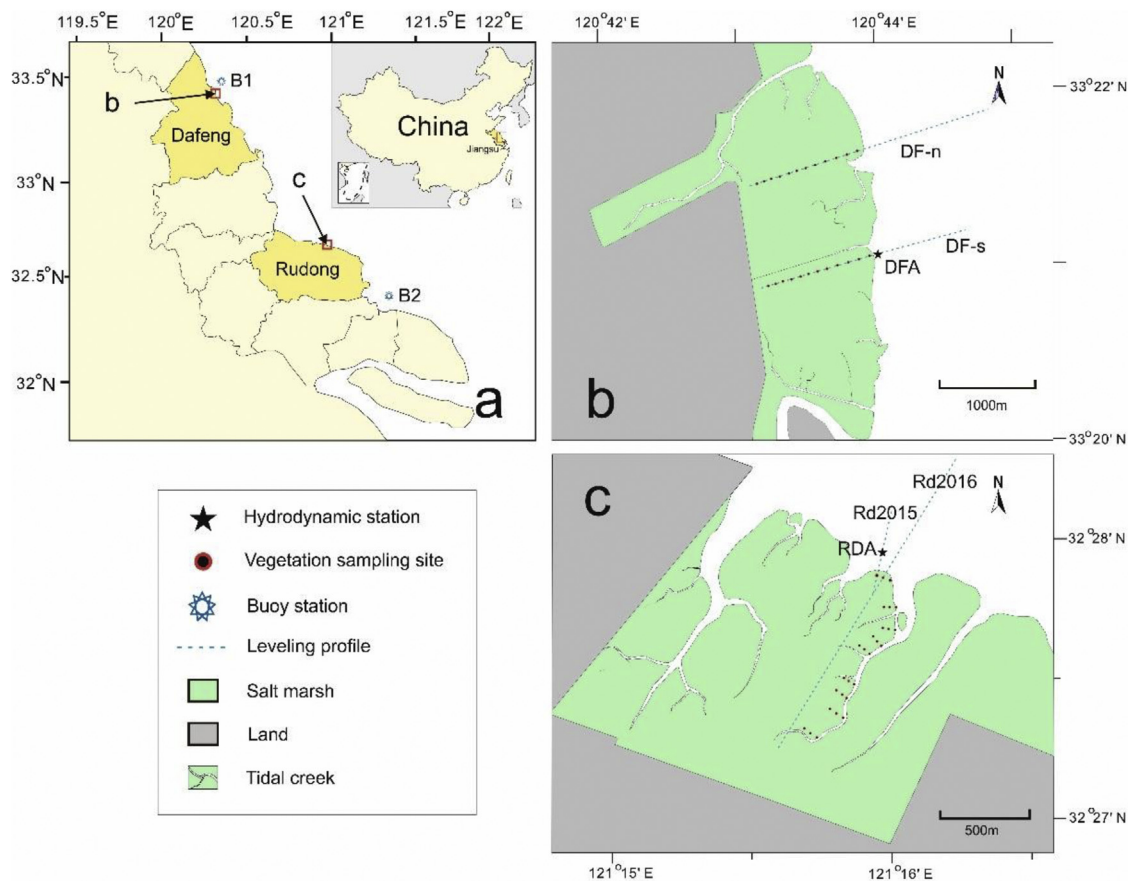


Fig. 1. (a): Map of the Dafeng and Rudong study areas, Jiangsu Province, China; B1 and B2 are buoy stations monitoring the wave climate. (b): The Dafeng salt marsh; DF-n and DF-s mark the two cross-shore profiles. (c): The Rudong salt marsh; Rd2015 and Rd2016 are the two transects along which elevation measurements were carried out in 2015 and 2016 respectively. DFA and RDA mark the locations of hydrodynamic measuring stations.

buoy; Fig. 1a). The Rudong coast, by contrast, while being exposed to stronger tidal currents, is shielded from wave action by the radial sand ridges which emerge during low tide. Correspondingly, the annual mean significant wave height measured at the B2 buoy (Fig. 1a), which is located in a similar morphological environment close to Rudong, is 0.27 m.

After its introduction to China, *S. alterniflora* rapidly expanded along the Jiangsu coast, landward up to the local native marsh communities and seaward across the bare tidal flat. By 2007 the *S. alterniflora* salt marsh occupied an area of 187.1 km² (Zuo et al., 2012). It showed excellent ecological engineering qualities with respect to sediment capture, shoreline protection and biological treatment of wastewater (Ding et al., 2008; Li et al., 2009; Zhang et al., 2012; Zuo et al., 2012). Because of its expansion in the course of land claims, the *S. alterniflora* marshes in Dafeng and Rudong can be regarded as representing single species marshes. Their landward edges are determined by dikes, whereas their seaward edges are lined by bare tidal flats.

2.2. Field surveys

Field surveys were carried out in Dafeng from 11–19 November 2016 and in Rudong from 24 September to 8 October 2015 and 24–25 October 2016. The two research sites represent typical *S. alterniflora* salt marshes along the Jiangsu coast. In Dafeng the marsh is lined by re-creating rise in an upper mesotidal environment, whereas in Rudong the marsh thrives in a lower macrotidal environment. The cross-shore profiles and vegetation patterns, however, differ between Dafeng and Rudong. As a consequence, elevation measurements and vegetation sampling were adapted to the local bed elevation profiles.

2.2.1. Bed elevation measurements

A Magellan Z-MAX GPS RTK (a differential, real-time kinematic GPS system) was used to measure bed elevations and positions. The instrument has a vertical accuracy of 20 mm. In each case, the GPS was allowed to stabilize for 3 s in order to optimize the elevation accuracy. The two bed leveling profiles at Dafeng were measured in November 2016 (Fig. 1b, transects DF-n and DF-s). The interval between two successive sampling points was in general 25 m. Vertical elevation changes were in all cases smaller than 5 cm. Only at rise and along tidal creeks were the sampling intervals reduced. A short profile was measured across the seaward edge of the marsh at Rudong in September 2015 (Fig. 1c, transect Rd2015). Because of the steeper slope beyond the seaward edge of the marsh, the interval between successive elevation measurements was decreased to 5 m, corresponding elevation changes being smaller than 3 cm. A second, supplementary profile with larger sampling intervals (50 m) was surveyed in October 2016 (Fig. 1c, transect Rd2016), the vertical elevation changes between points being smaller than 5 cm.

2.2.2. Vegetation sampling

According to Gao et al. (2016), the peak season of biomass is October in Jiangsu Coast. The biomass obtained at this peak season is able to represent the annual biomass. At Rudong the above-ground vegetation samples were collected in October 2015 and at Dafeng in November 2016. Both transects were sampled at Dafeng (Fig. 1b). In each case 12 quadrats (50*50 cm) spaced 100 m apart were collected. All above-ground plants in a quadrat were harvested. In addition, 3 quadrats at 0, 50, 100 m distance were collected along 8 transects perpendicular to a tidal creek at Rudong (Fig. 1c). The elevation and

position of each quadrat was measured by the RTK-GPS. The stem heights of all plants were measured in the lab before they were dried and weighed.

2.3. Laboratory analysis and data processing

The inundation ratio (*IR*) was calculated on the basis of the water level time series and the elevations. The water surface was assumed to be horizontal over the whole salt marsh (Friedrichs and Aubrey, 1996). The time series were obtained from the tidal gauges at Yangkou Harbor, 15 km from the Rudong site, and at Dafeng Harbor, 12 km from the Dafeng site. Inundation was defined as the case where the water surface elevation at a particular point was higher than the ground elevation. For all those cases the inundation ratio was calculated by eq. (3).

3. Results

3.1. Elevation

The actual accuracy of the elevation measurements was on average 43 mm. According to these, a low rise occurs between the marsh and the bare tidal flat at Dafeng. The height of the rise was 10 cm along transect DF-n and 65 cm along transect DF-s (Fig. 2a and b) and thus increases from north to south (Fig. 1b). Ground elevations across the marsh were almost at the same level at Dafeng (Fig. 2a and b), the marsh platform being slightly higher than MHW (1.50 m above MSL). According to our observations, the seaward edge of the salt marsh was eroding and hence retreating landward at Dafeng.

A rise was not observed at Rudong during the two field campaigns in 2015 and 2016. Here, the salt marsh was located below the MHW level (2.23 m above MSL). The slope of the seaward part of the marsh was 0.6%, that of the landward part and the bare tidal flat about 0.1% (Fig. 2c). The variations in ground elevation obviously imply different inundation ratios along the marsh profile. Furthermore, the elevations of vegetation quadrats near the tidal creek were found to be lower than those within the marsh (Fig. 2c).

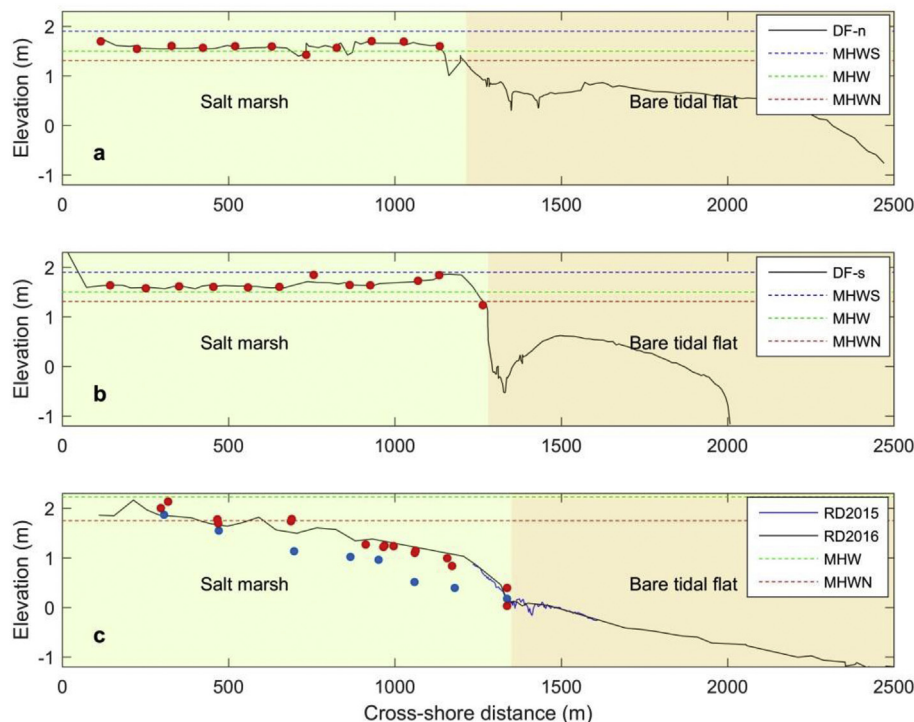


Fig. 2. Cross-shore elevation profiles at Dafeng and Rudong. MHW, MHWS, MHWN are mean high water, mean high water springs and mean high water neaps respectively. Elevation is relative to MSL. (a) & (b) The cross-shore elevation profiles at Dafeng. MHWS, MHW, MHWN are 1.91 m, 1.50 m and 1.31 m above MSL respectively. (c) The cross-shore elevation profile at Rudong. MHWS, MHW, MHWN are 2.84 m, 2.23 m and 1.75 m above MSL respectively. Red solid circles mark the vegetation sampling quadrats located within the marsh, the blue solid circles the quadrats near the tidal creek. (For interpretation of the references to colour in this figure legend, the reader is referred to the Web version of this article.)

3.2. Vegetation

3.2.1. Stem density and height

The marshes of Dafeng and Rudong are single species marshes. Only *S. alterniflora* was observed on the marsh during the field surveys. Stem density at Dafeng has two peaks, one at the seaward edge, the other 1000 m from the seaward edge of the marsh (Fig. 3b). Vegetation is dense (420 plants/m²) at the seaward edge of marsh, which corresponds to a high inundation ratio. The second peak (550 plants/m²) results from the gentle slope and concave-up shape of cross-shore elevation profile, which causes the middle part of marsh to be poorly drained and the upper marsh to be inundated for a longer period of time (Fig. 2a and b). At Rudong the stem density shows different pattern to Dafeng. The maximal stem density at the seaward edge of the marsh at Rudong is 540 plants/m², from where it decreases with increasing elevation toward the shore (Fig. 3a and b).

Stem height shows a parabolic relationship to elevation and cross-shore distance at both Rudong and Dafeng. The regression equation of stem height (*h_s*, m) versus elevation relative to MSL (*h*, m) is (Fig. 3c):

$$h_s = -41.41h^2 + 87.79h + 69.77 = -41.41*(h - 1.06)^2 + 116.3 \tag{4}$$

with a correlation coefficient of *R* = 0.47, whereas the regression equations of stem height (*h_s*, m) versus cross-shore landward distance from the seaward edge of the marsh (*L*, m) is (Fig. 3d):

$$h_s = -1*10^{-4}L^2 + 0.11L + 86.45 = -1*10^{-4}*(L - 550)^2 + 116.7 \tag{5}$$

with a correlations coefficient of *R* = 0.48. The hump-shaped curve reaches its highest elevation (1.1 m above MSL) at a distance of 550 m from the seaward edge (Fig. 3c and d). The maximal stem height is 159 cm. *S. alterniflora* is short at the seaward edge because short plants survive more easily under strong wave action and higher flow velocities. The plants on the landward side, in turn, are short due to the limiting effects of high salinity and drought. The most significant difference between the marshes at Dafeng and Rudong is their vertical growth range. While the marsh at Dafeng occupies a narrow elevation

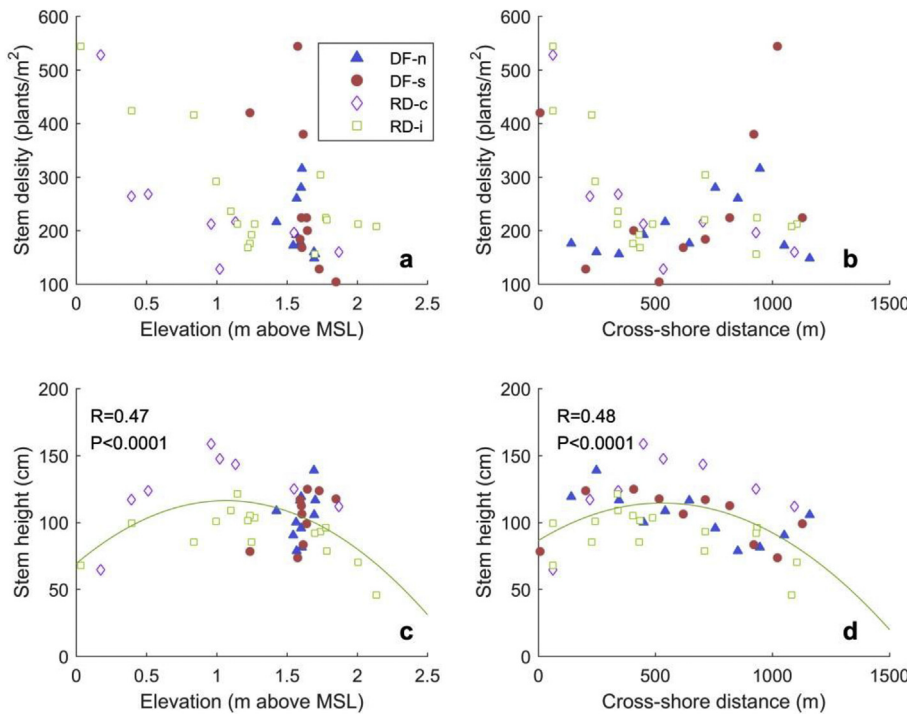


Fig. 3. Stem density and height versus elevation and cross-shore distance at Dafeng and Rudong. The cross-shore distance is landward from the seaward edge of the marsh. (a) & (b) Stem density versus Elevation and Cross-shore distance. Note the lack of correlation. (c) Stem height vs. Elevation, and. (d) Stem height vs. Cross-shore distance. For the corresponding equations and correlation coefficients of the latter two see text (eq. (4) and (5)). DF-n (blue solid triangles) and DF-s (red solid circles) mark samples from Dafeng; RD-c (purple open diamonds) mark samples near the tidal creek at Rudong; RD-i (green open squares) mark samples from the inner marsh at Rudong. (For interpretation of the references to colour in this figure legend, the reader is referred to the Web version of this article.)

range from 1.24 m to 1.85 m above MSL, the marsh at Rudong ranges from mean sea level up to 2.2 m above MSL (Fig. 3a, c).

3.2.2. Biomass and inundation ratio

The minimum and maximum biomasses at Dafeng were 1160 g/m² and 2650 g/m² respectively (Fig. 4a). The narrow vertical growth range of the *S. alterniflora* marsh at Dafeng (1.24–1.85 m above MSL) corresponds to IRs ranging from 0.32 to 0.091. The maximum biomass occurred at 1.5 m above MSL and had an IR of 0.18 (Figs. 4a and 5a). The minimum and maximum biomasses at Rudong, by contrast, were 350 g/m² and 2850 g/m² respectively (Fig. 4b). The wider vertical growth

range of the marsh at Rudong (2.1–0.3 m above MSL) corresponds to IRs ranging from 0.08 to 0.4. The maximum biomass occurred at 1.0 m above MSL and had an IR of 0.25 (Figs. 4b and 5b).

The relationship between biomass (g/m²) and elevation (h) as well as inundation ratio (IR) follows a parabolic trend at both Dafeng and Rudong (Figs. 4 and 5). However, the corresponding equations differ with respect to the values of the variables (Fig. 5). Thus, the equation of biomass vs. elevation for Dafeng is (Fig. 4a):

$$B = -8392.8 h^2 + 2.58 \times 10^4 h - 1.79 \times 10^4 = -8392.8 * (h - 1.54)^2 + 2002.0 \tag{6}$$

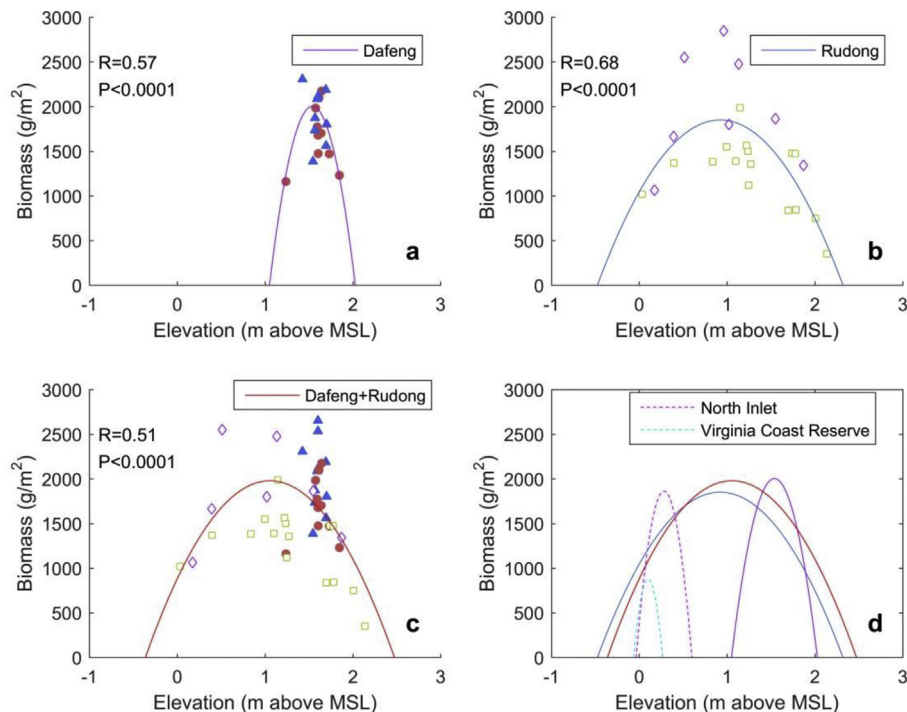


Fig. 4. Biomass versus elevation. Note the parabolic relationships for Dafeng (a), Rudong (b) and both together (c). For equations see text (eq. (6) and (7)). (d) The parabolic regressions of biomass vs. elevation at Dafeng and Rudong compared with those of North Inlet (South Carolina, USA) and the Virginia Coast Reserve (Virginia, USA). The latter data are from Morris et al. (2002) and Kirwan et al. (2012). For the equations of the latter two see text (eqs. (10) and (11)).

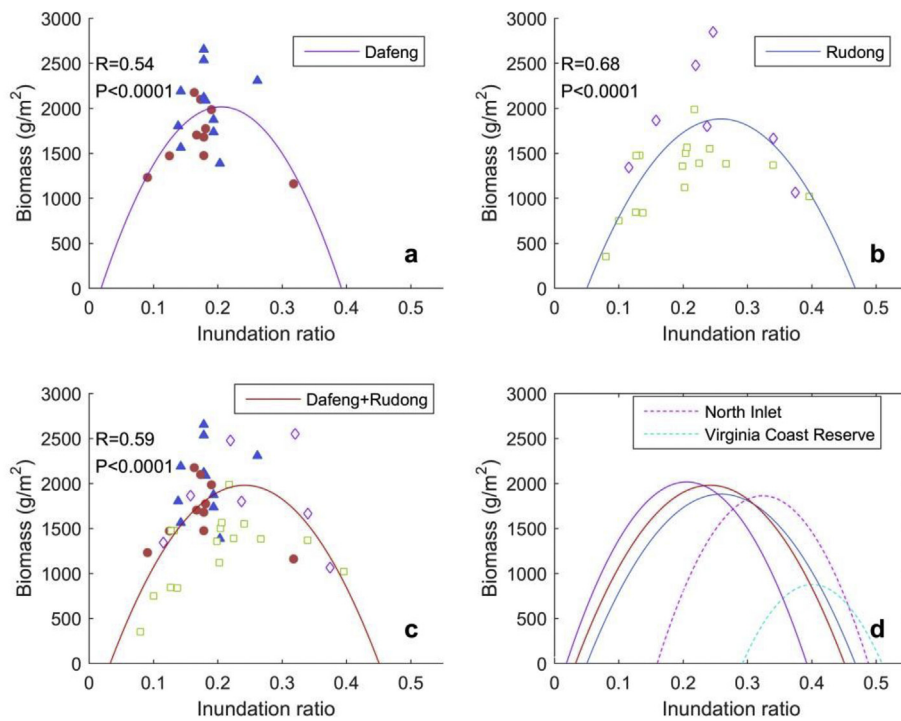


Fig. 5. Biomass versus inundation ratio. Note the parabolic relationships for Dafeng (a), Rudong (b) and both together (c). For equations see text (eq. (8) and (9)). (d) The parabolic regressions of biomass vs. inundation ratio at Dafeng and Rudong compared with those of North Inlet (South Carolina, USA) and the Virginia Coast Reserve (Virginia, USA). The latter data are from Morris et al. (2002) and Kirwan et al. (2012). For the equations of the latter two see text (eqs. (12) and (13)).

and for Rudong is (Fig. 4b):

$$B = -947.4 h^2 + 1743.2 h - 1048.3 = -947.4 * (h - 0.92)^2 + 1850.2 \tag{7}$$

According to these equations, the optimal elevation at Dafeng (1.54 m) is much higher than at Rudong (0.92 m). This reflects the wider growth range of the marsh at Rudong as compared to Dafeng.

In contrast to the biomass vs. elevation relationships, those of biomass vs. IR are quite similar at the two sites. Thus, the equation for Dafeng is (Fig. 5a):

$$B = -57796 IR^2 + 2.38 * 10^4 IR - 437.3 = -57796 * (IR - 0.206)^2 + 2015.3 \tag{8}$$

and that for Rudong is (Fig. 5b):

$$B = -43264 IR^2 + 2.25 * 10^4 IR - 1044.5 = -43264 * (IR - 0.26)^2 + 1880.1 \tag{9}$$

According to these equations, the optimal inundation ratio at Rudong (0.26) is slightly larger than that at Dafeng (0.206). Furthermore, the seaward IR limit at Dafeng (0.32) is smaller than that at Rudong (0.4).

4. Discussion

4.1. Tidal effect on vegetation growth

S. alterniflora is capable of tolerating stronger environmental stress than some other halophytes such as *Scirpus robustus*, *Scirpus mariqueter*, and *Spartina anglica* (Naidoo et al., 1992; Lewis et al., 2002; Chen et al., 2004; Wijte and Gallagher, 2013). This enables *S. alterniflora* to occupy elevation levels even below mean sea level (Wiggins and Binney, 1987; Landin, 1991; Bulthuis and Scott, 1993), although the precise seaward limits differ in different geographic regions (McKee and Patrick, 1988).

Parabolic relationships between biomass and elevation were reported from North Inlet (South Carolina, USA) and the Virginia Coast Reserve (Virginia, USA) (Morris et al., 2002; Kirwan et al., 2012). In order to compare the data between different study areas, all the data extracted from the literature need to be unified under a common

standard. Firstly, all reported elevations were related to mean sea level: $h = Z_{MHW} - D$, where h is the elevation relative to MSL, Z_{MHW} is the height between mean sea level and mean high water (mean tidal amplitude) and D is the depth of occurrence below mean high water. Second, time series of water level oscillations were obtained from regional tide-gauge records stored in the data base of NOAA (<https://tidesandcurrents.noaa.gov/datums.html?units=1&epoch=0&id=8632200&name=Kiptopeke&state=VA>). Thereafter, the inundation ratios can be calculated from the known water levels and elevations. The regression parameters from four area are listed in Table 1. The results from North Inlet and the Virginia Coast Reserve are displayed in Figs. 4d and 5d, and Table 2.

As can be seen, the growth ranges and optimal positions are very different between the marshes of Dafeng, Rudong, North Inlet and the Virginia Coast Reserve (Figs. 4d and 5d, Table 1). Whereas the biomass of *S. alterniflora* is similar in North Inlet and along the Jiangsu coast (maximal 2000 g/m³), it is much smaller in the Virginia Coast Reserve (maximal 800 g/m³). Thus, the respective equations of biomass vs. elevation for North Inlet and the Virginia Coast Reserve are

$$B = -18486 * (h - 0.28)^2 + 1861.6 \tag{10}$$

$$B = -32000 * (h - 0.10)^2 + 876.1 \tag{11}$$

and of biomass vs. inundation ratio:

$$B = -69161 * (IR - 0.324)^2 + 1861.7 \tag{12}$$

$$B = -74676 * (IR - 0.401)^2 + 875.5 \tag{13}$$

Table 1

Regression parameters of $B = a * (IR - b)^2 + c$, B (g/m²) is the biomass per unit area, IR is dimensionless inundation ratio, a , b and c are regression parameters.

Location	a	b	c	R	Significance
Dafeng	-57796	-0.206	2015.3	0.54	p < 0.001
Rudong	-43264	-0.260	1880.1	0.68	P < 0.001
North Inlet ^a	-69161	-0.324	1861.7	0.67	P < 0.001
Virginia Coast Reserve ^b	-74676	-0.401	875.5	0.65	P < 0.001

^a Data extracted from Morris et al. (2002).

^b Data extracted from Kirwan et al. (2012).

Table 2
Inundation ratios of different geographic regions.

	Rudong	Dafeng	North Inlet ^a	Virginia Coast Reserve ^b
Predicted seaward limit	0.47	0.39	0.49	0.54
Measured seaward limit	0.4	0.32	0.43	0.51
Predicted landward limit	0.04	0.02	0.16	0.28
Measured landward limit	0.08	0.1	0.19	0.34
Optimal <i>IR</i> of equation	0.26	0.206	0.324	0.401
Predicted growth range	0.43	0.37	0.33	0.23
Measured growth range	0.32	0.22	0.24	0.17
Tidal range (m)	4.5	3.0	1.4	0.8
Salt marsh slope	0.1%	~0%	/	3%
Latitude	32.5	33.3	33.3	37.5

Predicted values refer to those calculated by means of the corresponding equations relating biomass and *IR* to each other (eqs. (8), (9), (12) and (13)).

^a Data extracted from Morris et al. (2002).

^b Data extracted from Kirwan et al. (2012).

The seaward edges of the marsh in North Inlet and the Virginia Coast Reserve approximates mean sea level and the inundation ratio is about 0.5. Along the Jiangsu coast the seaward limit of the marsh is located slightly lower than in North Inlet and the Virginia Coast Reserve, but the submergence duration is smaller, being reversed due to the larger tidal ranges (Figs. 4d and 5d). The landward edge of the marsh along the Jiangsu coast, on the other hand, is significantly higher than in North Inlet and the Virginia Coast Reserve (Figs. 4d and 5d), while the *IR* value of the landward and seaward limits decrease with tidal range (Table 2). The optimal *IR* values at Dafeng, Rudong, North Inlet and the Virginia Coast Reserve are 0.206, 0.26, 0.35 and 0.41, respectively (Fig. 5d, Table 2). This demonstrates that the optimal *IR* value also tends to decrease with tidal range.

The elevation of the seaward limit along the Jiangsu coast is the lowest, and that in the Virginia Coast Reserve (Kirwan et al., 2012) the highest (Table 2). Introduced and hybrid plants may change the tolerance of *S. alterniflora* (Strong and Ayres, 2013), but differences in tidal range provide another explanation to this phenomenon. The growth range increase with increasing tidal range, whereas the landward and seaward limits decrease with increasing tidal range (McKee and Patrick, 1988). Biomass of *S. alterniflora* can be influenced by latitude (Liu et al., 2016; Crosby et al., 2017), but no significant difference was observed between 32 and 38° North (Liu et al., 2016). We assume that the submergence period and salinity tolerance is similar in these areas, which eliminates the effect of hybrids and latitude. While the inundation ratio in different geographic regions can be identical, the submergence depth will differ if the tidal range is different. Deeper submergence due to larger tidal ranges leads to stronger soil anoxia, which is unfavorable for the vegetation of the lower marsh. On the landward side, however, deeper submergence enhances inundation which is otherwise lacking in the higher marsh. Thus, submergence depth explains why both landward and seaward limits decrease with increasing tidal range (Fig. 5d, Table 2). Likewise, the inundation depth can explain the optimal *IR* value of vegetation growth. Submergence depth in microtidal environments will be shallower, and vegetation growth thus needs longer inundation durations to achieve higher inundation ratios.

Another remarkable phenomenon is that, with increasing tidal range, the landward limit decreases much more rapidly than the seaward limit (Fig. 5d, Table 2). Because the seaward edge of a marsh is regularly submerged, soil anoxia is mainly controlled by inundation duration not submergence depth. That explains why the seaward edge of a marsh varies much less between different areas than the landward edge, where the high marsh is irregularly submerged and evapotranspiration and hyper-salinity become severe. The effect of inundation duration, by contrast, is small because of its short duration and

submergence depth now becomes important. In effect, the response of the landward limit is much greater than that of the seaward limit if the tidal range changes. The same phenomenon, namely that the optimal *IR* decreases with tidal range, is also valid for the optimal *IR* of *S. alterniflora* growth.

4.2. Geomorphological effect on vegetation growth

Considering the observations at Dafeng and Rudong, the situation is more complicated than outlined above. The relationship of biomass and inundation frequency is similar at the two locations. The seaward *IR* limits are both smaller than 0.5, which concerns the elevation of the seaward edges of the marsh above mean sea level. It is determined by salinity and submergence tolerance of *S. alterniflora*. Although the tidal range at Dafeng is smaller than at Rudong, the seaward limit and the optimal *IR* value is smaller at Dafeng than at Rudong (Table 2). Hydrodynamics and geomorphology play important roles in this case. Firstly, at Dafeng the marsh edge retreats landward due to rise erosion. Secondly, due to the presence of the cliff, wave and current action are more intense (Tonelli et al., 2010; Francalanci et al., 2013; Zhao et al., 2017), which is a disadvantage for the vegetation. In response, the optimal *IR* position retreats to a higher elevation and therefore has a lower value.

By the same token, the cross-shore profile of a salt marsh may also alter the inundation characteristics. First of all, the marsh platform at Dafeng is located around MHW, which is much higher than the marsh at Rudong (Fig. 2). As mentioned above, the gentle slope and concave-up shape of the marsh at Dafeng (Fig. 2a and b) leads to poor drainage of the higher marsh. Because of the longer inundation duration, the soil salinity is lower, which favors vegetation growth of the higher marsh plants.

Tidal creeks are another landform influencing the vegetation pattern. Biomass and stem height of *S. alterniflora* located near the tidal creek (Figs. 3c, 4b and 5b) are clearly higher than on the inner marsh. The lower elevation near tidal creeks leads to higher inundation durations. While tidal creeks play an important role as drainage tunnels in salt marshes (Allen, 2000), the longer water residence times in their vicinity favor vegetation growth.

4.3. Salt marsh evolution and model application

As outlined above, the biomass model is clearly an important module in the geomorphological evolution model (Mudd et al., 2004, 2010; D'Alpaos et al., 2005, 2007; Morris, 2006; Kirwan and Murray, 2007; Mariotti and Fagherazzi, 2010). In the case of some *S. alterniflora* (Mudd et al., 2004, 2010; D'Alpaos et al., 2005, 2007) and multi-species marshes (Belliard et al., 2017) a linear equation can be used in the biomass model. The marshes at Dafeng and Rudong represent two kinds of typical marsh, being characterized by erosion along the cliff and a gentle slope with little or no surface deposition in the former case, but by seaward progression and a steep slope of the seaward edge in the latter case. As such, the marshes of Dafeng and Rudong can be regarded as representing two different evolutionary states.

Submergence has a positive effect on vegetation growth above the optimal *IR* elevation. The linear equation covers this part of the marsh up to the landward limit and provides an efficient predictor of biomass which, in this region, increases with decreasing elevation (Mudd et al., 2004, 2010; D'Alpaos et al., 2005, 2007). With seaward spreading of the vegetation, the frequency of submergence begins to inhibit the growth of *S. alterniflora*. The biomass decreases with decreasing elevation from the optimal elevation to the seaward limit. Here, the vegetation pattern follows a parabolic relationship between biomass and elevation. Because of decreased hydrodynamics and the sediment trapping effect of the salt marsh vegetation, the elevation of the entire marsh increases, whereas the slope of the inner marsh decreases and that of the seaward edge increases. As time goes on, the slope of the

seaward edge becomes progressively steeper until a cliff is formed. The period of cliff formation is significantly affected by sediment supply, biomass and overall evolution time (Mariotti and Fagherazzi, 2010; Zhao et al., 2017). The marshes of both the Dafeng and Rudong coasts are associated with high sediment concentrations (SSCs) and large biomass (Table 2). The different variables in the biomass versus *IR* relationship (e.g., optimal *IR*, landward and seaward *IR* limits, maximum biomass) can thus substantially influence morphodynamic processes, and are hence extremely important for morphological modeling and the development of management strategies for coastal marsh protection.

4.4. Salt marsh evolution under sea-level rise

According to the IPCC prediction of sea-level rise (SLR), the eustatic contribution will be 0.3–0.8 m over the next century (Church et al., 2013). In general terms, coastal land loss will occur if the local rate of SLR exceeds the local accretion rate (Reed, 1995). However, marsh survival may be different because of biogeomorphic feedbacks resulting in increased rates of both organic and inorganic accumulation (Morris et al., 2002; Kirwan and Guntenspergen, 2012). Thus, the spatial vegetation pattern is crucial in determining accumulation in the marsh, a dense plant canopy and associated high biomass greatly reducing the vulnerability of a marsh (Kirwan et al., 2016a,b). A maximal biomass and optimal marsh elevation would have the best protection effect. For example, at Dafeng and Rudong, and in North Inlet and the Virginia Coast Reserve, the respective maximal biomasses are 2002, 1850, 1861 and 875 g/m². The corresponding optimal elevations are 1.54, 0.92, 0.28, and 0.10 m above MSL, and the optimal *IR*s are 0.206, 0.260, 0.324 and 0.401.

The remarkable differences between different marshes will result in different responses to SLR. Because the *IR* of seaward edges are close to 0.5 in different regions, the associated lower optimal *IR* means that the marshes at higher elevations and with wider elevation ranges have a better chance to survive. The above-mentioned advantage of a marsh results in a stronger buffer to the impact of future SLR. Therefore, a maximal biomass and optimal *IR* are useful proxies in evaluating the ability of marsh adaptation to SLR. It is noteworthy, however, that the spatial pattern of a marsh is not the only determining factor, sediment supply being also a significant variable in the accretion of a marsh.

5. Conclusions

The biomass pattern of *S. alterniflora* in coastal marshes can be predicted by the inundation ratio. According to our field surveys, the relationships between above-ground biomass and inundation ratios can be described by quadratic regression equations. The optimal inundation ratio for *S. alterniflora* along the Jiangsu coast ranges from 0.21 to 0.26, but are much lower for the marsh in North Inlet (0.35) and the Virginia Coast Reserve (0.41). Similar differences apply to the landward and seaward limits of *S. alterniflora*. Tidal range plays a significant role in that larger tidal ranges lead to smaller optimal *IR*s and higher ground elevations at the landward and seaward limits of the marsh.

In addition, the landform of a salt marsh can also influence the growth pattern of *S. alterniflora*, while geomorphological factors such as the elevation profile, as well as the presence of cliffs and tidal creeks, should also be taken into account. Thus, the erosion of cliffs at Dafeng results in a higher seaward limit of the marsh. The gentle slope and concave-up shape of the Dafeng marsh, in turn, results in poor drainage, which makes the higher marsh more suitable for *S. alterniflora* than the better drained lower ground.

Acknowledgements

We thank the editor and reviewers for their constructive suggestions and comments. We are grateful to Yangyang Zhao, Baoming Yang, Tingfei Lan and Hao Wu for their participation in the field work. This

study was supported by the Natural Science Foundation of China (NSFC 41676077, 41676081), and the Fundamental Research Funds for the Central Universities (Grant No. 2016B00814).

Appendix A. Supplementary data

Supplementary data related to this article can be found at <https://doi.org/10.1016/j.ecss.2018.08.027>.

References

- Allen, J.R.L., 2000. Morphodynamics of holocene salt marshes: a review sketch from the atlantic and southern north sea coasts of europe. *Quat. Sci. Rev.* 19, 1155–1231.
- Alizad, K., Hagen, S.C., Morris, J.T., Bacopoulos, P., Bilskie, M.V., Weishampel, J.F., Medeiros, S.C., 2016. A coupled, two-dimensional hydrodynamic-marsh model with biological feedback. *Ecol. Model.* 327, 29–43.
- Balke, T., Stock, M., Jensen, K., Bouma, T.J., Kleyer, M., 2016. A global analysis of the seaward salt marsh extent: the importance of tidal range. *Water Resour. Res.* 52, 3775–3786.
- Belliard, J.P., Temmerman, S., Toffolon, M., 2017. Ecogeomorphic relations between marsh surface elevation and vegetation properties in a temperate multi-species salt marsh. *Earth Surf. Process. Landforms* 42, 855–865.
- Bertness, M.D., Ellison, A.M., 1987. Determinants of pattern in a New England salt marsh plant community. *Ecol. Monogr.* 57 (2), 129–147.
- Bockelmann, A.C., Bakker, J.P., Neuhaus, R., Lage, J., 2002. The relation between vegetation zonation, elevation and inundation frequency in a Wadden Sea salt marsh. *Aquat. Bot.* 73, 211–221.
- Bouma, T.J., van Duren, L.A., Temmerman, S., Claverie, T., Blanco-García, A., Ysebaert, T., Herman, P.M.J., 2007. Spatial flow and sedimentation patterns within patches of epibenthic structures: combining field, flume and modelling experiments. *Continental Shelf Res.* 27, 1020–1045.
- Bulthuis, D.A., Scott, B.A., 1993. Effects of Application of Glyphosate on Cordgrass, *Spartina Alterniflora*, and Adjacent Native Salt Marsh Vegetation in Padilla Bay, Washington. Padilla Bay National Estuarine Research Reserve, Shorelands and Coastal Zone Management Program. Washington State Department of Ecology.
- Chen, Y.N., Gao, S., Jia, J.J., Wang, A.J., 2005. Tidal ecological changes by transplanting *Spartina anglica* and *Spartina alterniflora*, northern Jiangsu coast. *Oceanol. Limnol. Sinica* 36, 394–403.
- Chen, Y., Li, Y., Cai, T., Thompson, C., Li, Y., 2016. A comparison of bihydrodynamic interaction within mangrove and saltmarsh boundaries. *Earth Surf. Process. Landforms* 41, 1967–1979.
- Chen, Y., Li, Y., Thompson, C., Wang, X., Cai, T., Chang, Y., 2018. Differential sediment trapping abilities of mangrove and saltmarsh vegetation in a subtropical estuary. *Geomorphology* 318, 270–282.
- Chen, Z.Y., Li, B., Zhong, Y., Chen, J.K., 2004. Ecological consequences and management of *Spartina* spp. invasions in coastal ecosystems. *Chin. Biodivers.* 12 (2), 280–289.
- Chung, C.H., Zhuo, R.Z., 1985. Twenty two years of *Spartina anglica* Hubbard in China. *Nanjing Univ. Res. Adv. Spartina* 31–35.
- Church, J.A., et al., 2013. Sea level change. In: Stocker, T.F. (Ed.), *Climate Change 2013: the Physical Science Basis*, pp. 1137–1216.
- Crosby, S.C., Angus, A., Jennifer, M.A., Bertness, M.D., Deegan, L.A., Sibinga, N., Leslie, H.M., 2017. *Spartina alterniflora* biomass allocation and temperature: implications for salt marsh persistence with sea-level rise. *Estuar. Coast* 40 (1), 213–223.
- D'Alpaos, A., Lanzoni, S., Marani, M., Fagherazzi, S., Rinaldo, A., 2005. Tidal network ontogeny: channel initiation and early development. *J. Geophys. Res. Earth Surf.* 110, F2.
- D'Alpaos, A., Lanzoni, S., Marani, M., Rinaldo, A., 2007. Landscape evolution in tidal embayments: modeling the interplay of erosion, sedimentation, and vegetation dynamics. *J. Geophys. Res. Earth Surf.* 112, 1–17.
- Ding, J., Mack, R.N., Lu, P., Ren, M., Huang, H., 2008. China's booming economy is sparking and accelerating biological invasions. *Bioscience* 58, 317–324.
- Feagin, R.A., Irish, J.L., Möller, I., Williams, A.M., Colón-Rivera, R.J., Mousavi, M.E., 2011. Engineering properties of wetland plants with application to wave attenuation. *Ecol. Eng.* 58, 251–255.
- Francalanci, S., Bondoni, M., Rinaldi, M., Solari, L., 2013. Ecomorphodynamic evolution of salt marshes: experimental observations of bank retreat processes. *Geomorphology* 195, 53–65.
- Friedrichs, C.T., Aubrey, D.G., 1996. Uniform bottom shear stress and equilibrium hypsometry of intertidal flats. In: In: Pattiaratchi, C. (Ed.), *Mixing in Estuaries and Coastal Seas, Coastal and Estuarine Stud.*, vol. 50. AGU, Washington, D. C, pp. 405–429.
- Friedrichs, C.T., Perry, J.E., 2001. Tidal salt marsh morphodynamics: a synthesis. *J. Coast Res.* 7–37.
- Gallagher, J.L., Reimold, R.J., Linthurst, R.A., Pfeiffer, W.J., 1980. Aerial production, mortality, and mineral accumulation-export dynamics in *Spartina alterniflora* and *Juncus roemerianus* plant stands in a Georgia Salt Marsh. *Ecology* 61, 303–312.
- Gao, J.H., Feng, Z.X., Chen, L., Wang, Y.P., Bai, F., Li, J., 2016. The effect of biomass variations of *Spartina alterniflora* on the organic carbon content and composition of a salt marsh in northern Jiangsu Province, China. *Ecol. Eng.* 95, 160–170.
- Gao, S., Du, Y.F., Xie, W.J., Gao, W.H., Wang, D.D., Wu, X.D., 2014. Environment-ecosystem dynamic processes of *Spartina alterniflora* salt-marshes along the eastern China coastlines. *Sci. China Earth Sci.* 57, 2567–2586.

- Gray, A.J., 1992. Salt marsh plant ecology: zonation and succession revisited. In: Allen, J.R.L., Pye, K. (Eds.), *Salt Marshes – Morphodynamics, Conservation and Engineering Significance*. Cambridge University Press, Cambridge, pp. 63–79.
- Hagen, S.C., Morris, J.T., Bacopoulos, P., Weishampel, J.F., 2013. Sea-level rise impact on a salt marsh system of the lower St. Johns River. *J. Waterw. Port. Coast. Ocean Eng.* 139, 118–125.
- Kirwan, M.L., Murray, A.B., 2007. A coupled geomorphic and ecological model of tidal marsh evolution. *Proc. Natl. Acad. Sci.* 104, 6118–6122.
- Kirwan, M.L., Christian, R.R., Blum, L.K., Brinson, M.M., 2012. On the relationship between sea level and *Spartina alterniflora* production. *Ecosystems* 15 (1), 140–147.
- Kirwan, M.L., Guntenspergen, G.R., 2012. Feedbacks between inundation, root production, and shoot growth in a rapidly submerging brackish marsh. *J. Ecol.* 100, 764–770.
- Kirwan, M.L., Walters, D.C., Reay, W.G., Carr, J.A., 2016a. Sea level driven marsh expansion in a coupled model of marsh erosion and migration. *Geophys. Res. Lett.* 43, 4366–4373.
- Kirwan, M.L., Temmerman, S., Skeehan, E.E., Guntenspergen, G.R., Fagherazzi, S., 2016b. Overestimation of marsh vulnerability to sea level rise. *Nat. Clim. Change* 6 (3), 253–260.
- Landin, M.C., 1991. Growth habits and other considerations of smooth cordgrass, *Spartina alterniflora* Loisel. In: *Spartina Workshop Record*. Washington Sea Grant Program. University of Washington, Seattle, pp. 15–20.
- Lewis, M.A., Weber, D.L., Moore, J.C., 2002. An Evaluation of the use of colonized periphyton as an indicator of wastewater impact in near-coastal areas of the Gulf of Mexico. *Arch. Environ. Contam. Toxicol.* 43, 11–18.
- Li, B., Liao, C.H., Zhang, X.D., Chen, H.L., Wang, Q., Chen, Z.Y., Gan, X.J., 2009. *Spartina alterniflora* invasions in the Yangtze River estuary, China: an overview of current status and ecosystem effects. *Ecol. Eng.* 35, 511–520.
- Liu, W., Douglass, K.M., Strong, D.R., Pennings, S.C., Zhang, Y.H., 2016. Geographical variation in vegetative growth and sexual reproduction of the invasive *Spartina alterniflora* in China. *J. Ecol.* 104, 173–181.
- Mariotti, G., Fagherazzi, S., 2010. A numerical model for the coupled long-term evolution of salt marshes and tidal flats. *J. Geophys. Res.* 115, 1–15.
- McKee, K.L., Patrick Jr., W.H., 1988. The relationship of smooth cordgrass to tidal (*Spartina alterniflora*) Datums: a review. *Estuaries* 11, 143–151.
- Morris, J.T., 1995. The mass balance of salt and water in intertidal sediments: results from north inlet, South Carolina. *Estuaries* 18, 556.
- Morris, J.T., 2006. Competition among marsh macrophytes by means of geomorphological displacement in the intertidal zone. *Estuar. Coast Shelf Sci.* 69, 395–402.
- Morris, J.T., Sundareshwar, P.V., Nietch, C.T., Kjerfve, B., Cahoon, D.R., 2002. Responses of coastal wetlands to rising sea level. *Ecology* 83, 2869–2877.
- Morris, J.T., Haskin, B., 1990. A 5-yr record of aerial primary production and stand characteristics of *Spartina alterniflora*. *Ecology* 71, 2209–2217.
- Morris, J.T., 2000. Effects of sea level anomalies on estuarine processes. In: *Estuarine Science: a Synthetic Approach to Research and Practice*. Island Press, Washington, DC, pp. 107–127.
- Morris, J.T., Sundberg, K., Hopkinson, C.S., 2013. Salt marsh primary production and its responses to relative sea level and nutrients in estuaries at Plum Island, Massachusetts, and North Inlet, South Carolina, USA. *Oceanography* 26, 78–84.
- Mudd, S.M., D'Alpaos, A., Morris, J.T., 2010. How does vegetation affect sedimentation on tidal marshes? Investigating particle capture and hydrodynamic controls on biologically mediated sedimentation. *J. Geophys. Res.* 115, F03029.
- Mudd, S.M., Fagherazzi, S., Morris, J.T., Furbish, D.J., 2004. Flow, Sedimentation, and Biomass Production on a Vegetated Salt Marsh in South Carolina: toward a Predictive Model of Marsh Morphologic and Ecologic Evolution. *The Ecogeomorphology of Tidal Marshes*. pp. 165–188.
- Mudd, S.M., Howell, S.M., Morris, J.T., 2009. Impact of dynamic feedbacks between sedimentation, sea-level rise, and biomass production on near-surface marsh stratigraphy and carbon accumulation. *Estuar. Coast Shelf Sci.* 82, 377–389.
- Naidoo, G., McKee, K.L., Mendelsohn, I.A., 1992. Anatomical and metabolic responses to waterlogging and salinity in *Spartina alterniflora* and *S. patens* (Poaceae). *Am. J. Bot.* 79, 765–770.
- Nepf, H.M., 2012. Flow and transport in regions with aquatic vegetation. *Annu. Rev. Fluid Mech.* 44, 123–142.
- Phleger, C.F., 1971. Effect of salinity on growth of a salt marsh grass. *Ecology* 52, 908–911.
- Ren, M.E., 1986. *Comprehensive Investigation of the Coastal Zone and Tidal Land Resources of Jiangsu Province*. Ocean Press, Beijing.
- Reed, D.J., 1995. The response of coastal marshes to sea-level rise: survival or submergence? *Earth Surf. Process. Landforms* 20, 39–48.
- Rodriguez, J., Saco, P.M., Sandi, S., Saintilan, N., Riccardi, G., 2017. Potential increase in coastal wetland vulnerability to sea-level rise suggested by considering hydrodynamic attenuation effects. *Nat. Commun.* 8, 16094.
- Shi, Z., Pethick, J.S., Pye, K., 1995. Flow structure in and above the various heights of a saltmarsh canopy: a laboratory flume study. *J. Coast Res.* 11, 1204–1209.
- Strong, D.R., Ayres, D.R., 2013. Ecological and evolutionary misadventures of *Spartina*. *Annu. Rev. Ecol. Syst.* 44, 389–410.
- Temmerman, S., Patrick, M., Bouma, T.J., Herman, P.M.J., Ysebaert, T., De Vriend, H.J., 2013. Ecosystem-based coastal defence in the face of global change. *Nature* 504, 79–83.
- Tonelli, M., Fagherazzi, S., Petti, M., 2010. Modeling wave impact on salt marsh boundaries. *J. Geophys. Res. Ocean.* 115, 1–17.
- Voss, C.M., Robert, R.C., Morris, J.T., 2013. Marsh macrophyte responses to inundation anticipate impacts of sea-level rise and indicate ongoing drowning of North Carolina marshes. *Mar. Biol.* 160, 181–194.
- Wang, A., Gao, S., Chen, J., Li, D., 2009. Sediment dynamic responses of coastal salt marsh to typhoon “KAEMI” in Quanzhou Bay, Fujian Province, China. *Chin. Sci. Bull.* 54, 120–130. <https://doi.org/10.1007/s11434-008-0365-7>.
- Wang, Y.P., Gao, S., Jia, J.J., Thompson, C.L., Gao, J.H., Yang, Y., 2012. Sediment transport over an accretional intertidal flat with influences of reclamation, Jiangsu coast, China. *Mar. Geol.* 291–294, 147–161.
- Wiggins, J., Binney, E.P., 1987. *A Baseline Study of the Distribution of Spartina Alterniflora in Padilla Bay*. Report to Washington State Department of Ecology, Padilla Bay National Estuarine Research Reserve.
- Wijte, A.H.B.M., Gallagher, J.L., 2013. Effect of oxygen availability and salinity on early life history stages of salt marsh plants. I. Different germination strategies of *Spartina alterniflora* and *Phragmites australis* (Poaceae). *Am. J. Bot.* 83, 1337–1342.
- Yang, S.L., 1998. The Role of *Scirpus* marsh in attenuation of hydrodynamics and retention of fine sediment in the Yangtze Estuary. *Estuar. Coast Shelf Sci.* 47, 227–233.
- Yang, S.L., Shi, B.W., Bouma, T.J., Ysebaert, T., Luo, X.X., 2012. Wave attenuation at a salt marsh margin: a case study of an exposed coast on the yangtze estuary. *Estuar. Coast* 35, 169–182.
- Zhang, R.S., Shen, Y.M., Lu, L.Y., Yan, S.G., Wang, Y.H., Li, J.L., Zhang, Z.L., 2004. Formation of *Spartina alterniflora* salt marshes on the coast of Jiangsu Province, China. *Ecol. Eng.* 23, 95–105.
- Zhang, Y., Huang, G., Wang, W., Chen, L., Lin, G., 2012. Interactions between mangroves and exotic *Spartina* in an anthropogenically disturbed estuary in southern China. *Ecology* 93, 588–597.
- Zhao, Y., Yu, Q., Wang, D., Wang, Y.P., Wang, Y., Gao, S., 2017. Rapid formation of marsh-edge cliffs, Jiangsu coast, China. *Mar. Geol.* 385, 260–273.
- Zuo, P., Zhao, S., Liu, C., Wang, C., Liang, Y., 2012. Distribution of *Spartina spp.* along China's coast. *Ecol. Eng.* 40, 160–166.
- Zuo, P., Li, Y., Liu, C.A., Zhao, S.H., Guan, D.M., 2013. Coastal wetlands of China: changes from the 1970s to 2007 based on a new wetland classification system. *Estuar. Coast* 36, 390–400.